

perpendicular direction. For a polarized triton beam, a neutron flux of about  $8.4 \times 10^6$ /sec is obtained at any angle. Such fluxes compare very favorably with those available from the commonly used polarized neutron-source reactions. In addition, of course, polarization values attainable by the present technique are much higher. Yields could be greatly enhanced by the use of more sophisticated targets. For example, liquid-helium-cooled differentially pumped targets,  $D_2O$  ice, or  $T_2O$  ice targets might be considered. In addition, it is quite

possible that polarized ion currents substantially higher than  $1 \mu A$  will be realized in the next few years.

#### ACKNOWLEDGMENTS

I would like to thank W. Haerberli, P. W. Keaton, E. M. Bernstein, J. D. Seagrave, J. Simmons, and D. C. Dodder for helpful discussions. I would especially like to thank R. D. Cowan for the use of his FORTRAN IV subroutines for evaluating the Wigner 3- $j$ , 6- $j$ , and 9- $j$  symbols.

### Study of the $(d,p)$ Reaction in the $1p$ Shell\*

J. P. SCHIFFER, G. C. MORRISON, R. H. SIEMSEN,<sup>†</sup> AND B. ZEIDMAN

*Argonne National Laboratory, Argonne, Illinois*

(Received 3 August 1967)

Angular distributions for the  $(d,p)$  reaction leading to bound states in the  $1p$  shell have been obtained at  $E_d = 12$  MeV for all stable targets. Spectroscopic factors obtained in distorted-wave Born-approximation (DWBA) analyses with average parameters are in surprisingly good agreement with those obtained in the shell-model calculations of Cohen and Kurath. The oscillating structure of the angular distributions at backward angles tends to be qualitatively reproduced by the DWBA calculations, although the amplitudes of the oscillations and the magnitudes of the backward cross sections are very sensitive to details of the calculations.  $J$ -dependent effects, similar to those found in heavier nuclei, but with some complications, are also found here.

#### I. INTRODUCTION

THE study of  $(d,p)$  reactions on light nuclei dates back to the early days of plane-wave stripping theory.<sup>1</sup> The  $(d,p)$  reactions on  $1p$ -shell nuclei were then studied<sup>2</sup> at several energies in the cyclotron energy range  $\gtrsim 8$  MeV. The main purpose of these investigations was to assign the orbital angular momenta  $l$  of the transferred neutrons. Consequently, most of these early investigations were restricted to forward angles, since backward angles were not expected to contain any useful information. Similarly, many of the experiments reported only relative-cross sections, or rather poorly determined absolute ones, since the plane-wave Born-approximation (PWBA) stripping theories predict absolute yields which are too large by one to two orders of magnitude. The early work was summarized in the review article by Macfarlane and French.<sup>3</sup>

Since the introduction of the DWBA stripping theory, the interest has tended to shift to heavier nuclei, although a larger number of  $(d,p)$  and  $(d,n)$  experiments on light nuclei at  $E_d \lesssim 6$  MeV have also been interpreted by the DWBA with varying degrees of success. There have been relatively few studies of  $(d,p)$  reactions on  $1p$ -shell nuclei at energies above 6 MeV,<sup>4-11</sup> and most of these were on  $Be^9$ ,  $B^{10}$ , and  $C^{12}$  targets and led to ground states. As a consequence, the data were rather incomplete at these energies at which compound-nucleus effects might become relatively unimportant. This longtime neglect of the direct reactions on light nuclei probably reflects general misgivings regarding the applicability of optical-model potentials and the DWBA in light nuclei. It therefore seems somewhat

\* Work performed under the auspices of the U. S. Atomic Energy Commission.

<sup>†</sup> Present address: Nuclear Structure Laboratory, Yale University, New Haven, Connecticut.

<sup>1</sup> S. T. Butler, Proc. Roy. Soc. (London) **A208**, 559 (1951).

<sup>2</sup> J. R. Holt and T. N. Marsham, Proc. Phys. Soc. (London) **A66**, 1032 (1953); S. H. Levine, R. S. Bender, and J. N. McGruer, Phys. Rev. **97**, 1249 (1955); N. T. S. Evans and W. C. Parkinson, Proc. Phys. Soc. (London) **A67**, 684 (1954); J. Rotblat, Phys. Rev. **83**, 1271 (1951); J. R. Holt and T. N. Marsham, Proc. Phys. Soc. (London) **A66**, 258 (1953); W. M. Gibson and E. E. Thomas, *ibid.* **A210**, 543 (1951).

<sup>3</sup> M. H. Macfarlane and J. B. French, Rev. Mod. Phys. **32**, 567 (1960).

<sup>4</sup> S. Morita, N. Kawai, N. Takano, Y. Goto, R. Hanada, Y. Nakajima, S. Takemoto, and Y. Yaegashi, J. Phys. Soc. Japan **15**, 550 (1960).

<sup>5</sup> B. Zeidman, J. L. Yntema, and G. R. Satchler, in *Proceedings of the Rutherford Jubilee International Conference, Manchester, 1961*, edited by J. B. Birks (Heywood and Company Ltd., London, 1961), p. 515.

<sup>6</sup> S. Morita, T. Ishimatsu, T. Cho, Y. Nakajima, N. Kawai, T. Murata, and Y. Hachiya, J. Phys. Soc. Japan **16**, 1849 (1961).

<sup>7</sup> R. J. Slobodrian, Phys. Rev. **126**, 1059 (1962).

<sup>8</sup> S. Hinds and R. Middleton, Nucl. Phys. **38**, 114 (1962).

<sup>9</sup> R. van Dantzig and L. A. Ch. Koerts, Nucl. Phys. **48**, 177 (1963).

<sup>10</sup> U. Schmidt-Rohr, R. Stock, and P. Turek, Nucl. Phys. **53**, 77 (1964).

<sup>11</sup> L. L. Lee, Jr. and R. H. Siemssen, Bull. Am. Phys. Soc. **10**, 510 (1965); and (to be published).

surprising that in the present work, the spectroscopic data obtained from the  $(d, p)$  reaction on  $1p$ -shell nuclei are in quite good agreement with theoretical expectations.

In recent years several DWBA studies of  $(d, p)$  reactions on light nuclei have been published,<sup>5,12-14</sup> the most recent being that of Alty *et al.*<sup>15</sup> on the  $O^{16}(d, p)O^{17}$  reaction. (We again restrict our discussion to energies above 9 MeV). In all these investigations, the distorting potentials were obtained either by adjusting parameters to give a best fit to the measured  $(d, p)$  angular distributions, or by fitting elastic data for the appropriate nucleus and energy. The ambiguities associated with optical-model fits to elastic scattering at one energy or on one target are well known; the additional reasons for being suspicious of individual optical-model fits on light nuclei are numerous. In view of these difficulties we chose to make the rather arbitrary drastic restriction of using a fixed, average set of optical-model parameters for all the reactions studied.

In the present work we attempt to extract reduced transition probabilities within the  $1p$  shell from the  $(d, p)$  reaction on light nuclei, and we compare our results with the predictions of recent shell-model calculations. As an additional point of interest, we consider the details of the angular distribution from the point of view of the  $J$  dependence in the  $(d, p)$  reaction—which has been found to be quite pronounced in heavier nuclei for transitions within the  $2p$  shell.<sup>16</sup>

## II. EXPERIMENTAL METHODS AND RESULTS

Angular distributions and absolute cross sections for the  $(d, p)$  reactions on targets of  $Li^6$ ,  $Li^7$ ,  $B^{11}$ ,  $C^{12}$ ,  $C^{13}$ , and  $N^{14}$  were measured with 12.0-MeV deuterons accelerated by the Argonne tandem Van de Graaff. Most of the measurements were performed in an 18-in. scattering chamber<sup>17</sup> with surface-barrier detectors, but in some cases it was found advisable to use a broad-range spectrograph<sup>18</sup> with photographic emulsions.

### Targets

A variety of targets were used during the course of the experiment. The C targets consisted of self-supporting carbon films, either of natural abundance or enriched to  $\sim 52\%$   $C^{13}$ . The  $B^{11}$  targets were self-supporting, prepared from enriched  $B^{11}$  in a manner previously

described.<sup>19</sup> Lithium targets were made by evaporating enriched  $Li^6$  or  $Li^7$  onto thin ( $\sim 20 \mu\text{g}/\text{cm}^2$ ) carbon substrates in a bell jar. In order to reduce oxygen contamination, the Li targets were transferred through a vacuum lock and mounted in the scattering chamber under vacuum.  $N^{14}$  targets consisted of melamine evaporated onto a carbon substrate. Typical target thickness was  $\sim 300 \mu\text{g}/\text{cm}^2$ . In addition to the above targets, which were used for the  $(d, p)$  measurements, targets of  $CF_3$ ,  $LiF$ , and  $CaF_2$  were used in determination of absolute cross sections as discussed below.

### Particle Detection

In the scattering chamber, charged particles from the target were stopped in  $E(dE/dx)$  telescopes consisting of silicon surface-barrier detectors. The  $\Delta E$  counters were approximately  $150 \mu$  thick, while the  $E$  (stopping) counters were over  $2000 \mu$  thick. To facilitate data acquisition, two telescopes, separated by  $15^\circ$ , were mounted in the same holder. The entire detector mount was cooled by thermoelectric coolers to reduce detector leakage current and noise, and permanent magnets were used to suppress fast electrons from the target.<sup>20</sup> The physical arrangement permitted measurements over the angular range from  $10^\circ$  to  $165^\circ$  with respect to the incident-beam direction. Tantalum apertures placed before the counters defined the solid angle of the detector, which ranged from  $\sim 5 \times 10^{-4}$  sr at forward angles to  $1 \times 10^{-3}$  at back angles. In order to normalize the data between different runs and telescopes, spectra were recorded in both telescopes at several overlapping scattering angles. This normalization was accomplished through the use of a fixed-angle monitor counter which viewed reaction products from the particular nuclide being studied. The particle-selection circuit formed the product of the  $\Delta E$  and  $E$  signals to yield an output proportional to the mass of the particle.<sup>21</sup> Single-channel analyzers selecting the appropriate mass and energy ranges fed a coincidence circuit which gated a multichannel analyzer on which were recorded the total energy ( $E + \Delta E$ ) of the particle. The system used in this manner allowed detection, with particle selection, of protons with energy greater than 4.5 MeV or of deuterons with energies greater than 5.5 MeV. The energy resolution width of the system was about 100 keV, which usually was adequate for complete resolution of the states of interest.

Dead-time corrections were made by scaling the number of gates and the number of events recorded by the multichannel analyzer. An accurate dead-time correction was possible with counting rates resulting

<sup>12</sup> H. W. Barz, R. Fülle, D. Netzband, R. Reif, K. Schlott, and J. Slotta, Nucl. Phys. **73**, 473 (1965).

<sup>13</sup> W. R. Smith and E. V. Ivash, Phys. Rev. **131**, 304 (1963).

<sup>14</sup> R. van Dantzig and W. Tobocman, Phys. Rev. **136**, B1682 (1964).

<sup>15</sup> J. L. Alty, L. L. Green, R. Huby, G. D. Jones, J. R. Mines, and J. F. Sharpey-Schafer, Nucl. Phys. **A97**, 541 (1967).

<sup>16</sup> L. L. Lee, Jr. and J. P. Schiffer, Phys. Rev. **136**, B405 (1964).

<sup>17</sup> T. H. Braid and J. T. Heinrich (unpublished).

<sup>18</sup> J. R. Erskine, Phys. Rev. **135**, B110 (1964).

<sup>19</sup> J. R. Erskine and D. S. Gemmel, Nucl. Instr. Methods **24**, 397 (1963).

<sup>20</sup> E. D. Klema, L. L. Lee, Jr., and J. P. Schiffer, Phys. Rev. **161**, 1134 (1967).

<sup>21</sup> G. L. Miller and V. Radeka, Brookhaven National Laboratory Report No. BNL-6952 (unpublished); and IEEE Trans. Nucl. Sci. **11**, 302 (1964).

in analyzer dead times  $<10\%$ , since the analyzer was the slowest component of the system. In some cases contaminants in the target, mostly carbon and oxygen, produced peaks that interfered with the peaks of interest over significant intervals in the energy spectrum. In order to separate these peaks, it was necessary to use a broad-range magnetic spectrograph in which particles were detected in photographic emulsions. With the use of somewhat thinner targets, a substantial improvement in resolution was achieved. It was also found advisable to use the spectrograph for measurements at extreme forward angles where, in the counters, elastic scattering produced high counting rates that caused pile up and reactions in the Si.

### Absolute Cross Sections

A major difficulty in measurements of absolute cross sections is the determination of target thickness. This problem is particularly severe for light nuclei and evaporated targets, for which contaminants and the substrate may constitute a substantial fraction of the total target thickness. However, the effective thickness of a particular target can be determined by measuring a reaction with a known cross section. In actual practice, absolute  $(d,p)$  cross sections were obtained by direct comparison with the known cross sections without requiring that the detector solid angle, the beam

charge, and the target thickness be known. For  $B^{11}$  and  $N^{14}$ , the relative values were compared with the known cross sections<sup>22</sup> for elastic scattering from these nuclei at  $E_d=11.8$  MeV.<sup>23</sup> For  $Li^6$ ,  $Li^7$ , and  $C^{12}$ , the cross sections were obtained by using  $LiF$  and  $CF_2$  targets. The yield of elastic deuterons was compared with that from pure elemental targets and with that obtained from a  $CaF_2$  target. The measured cross section of deuterons elastically scattered from  $Ca^{40}$  was then used<sup>24</sup> together with the known chemical composition of the targets to obtain absolute cross sections. For  $C^{13}$ , the cross section was obtained relative to  $C^{12}$  with a natural carbon target. For  $Be^9$ , the  $(d,p)$  cross section at extreme forward angles was measured at 12.0 MeV relative to the 11.8-MeV Heidelberg measurement<sup>10</sup> at  $55^\circ$ , because at extreme forward angles there were large uncertainties in the results at 11.8 MeV.

The experimental angular distributions are plotted in Figs. 1–3 and are presented in tabular form in the Appendix. The results on  $Be^9$  and  $B^{10}$  are those of Refs. 10 and 11, respectively, except that the peak cross sections have been remeasured here for  $Be^9$ . The peak cross sections are summarized in Table I. It is estimated that the absolute values of the cross sections measured in the present experiment are accurate to 15%; this includes statistical errors as well as our estimates of systematic error.

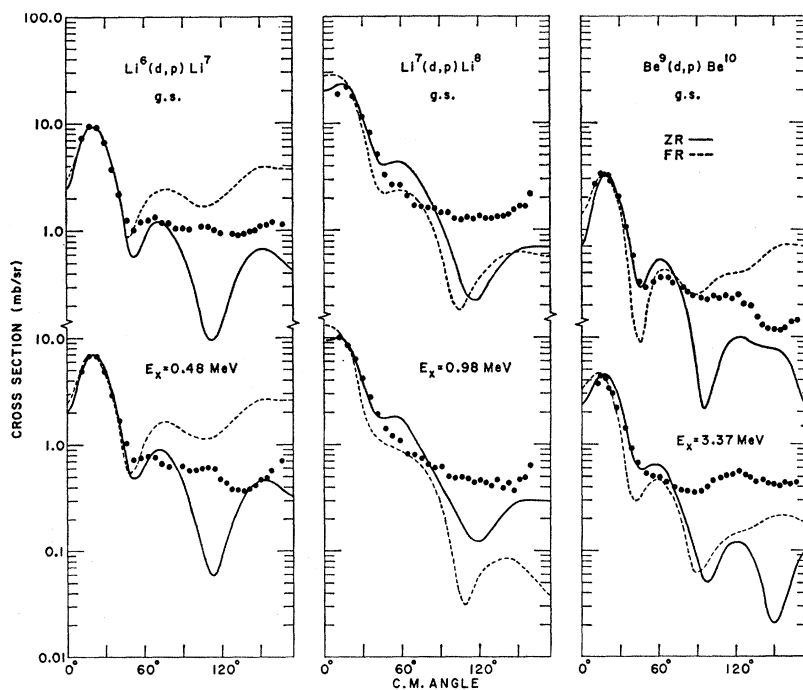


FIG. 1. Measured angular distributions of the  $(d,p)$  reaction from  $Li^6$ ,  $Li^7$ , and  $Be^9$  targets. The data on  $Li$  were obtained at 12 MeV, those on  $Be^9$  are from Ref. 10. The lines represent DWBA calculations as described in the text. The solid lines are for zero range, the dashed for finite range (local-energy approximation, LEA).

<sup>22</sup> W. Fitz, R. Jahr, and R. Santo, Nucl. Phys. **A101**, 449 (1967).

<sup>23</sup> It should be noted that the cross section initially chosen for  $N^{14}$  was that of Gibson and Thomas (Ref. 2). However, this was found to be in error by more than an order of magnitude.

<sup>24</sup> R. H. Bassel, R. M. Drisko, G. R. Satchler, L. L. Lee, Jr., J. P. Schiffer, and B. Zeidman, Phys. Rev. **136**, B971 (1964).

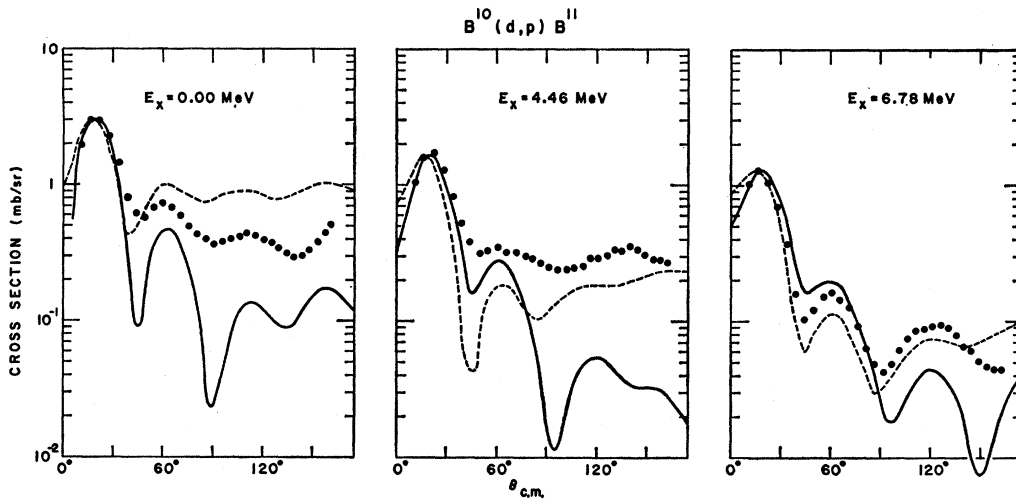


FIG. 2. Measured angular distributions of the  $B^{10}(d,p)B^{11}$  reaction at 12 MeV, taken from Ref. 11. The curves represent zero-range (solid) and finite range (dashed) DWBA calculations as described in the text.

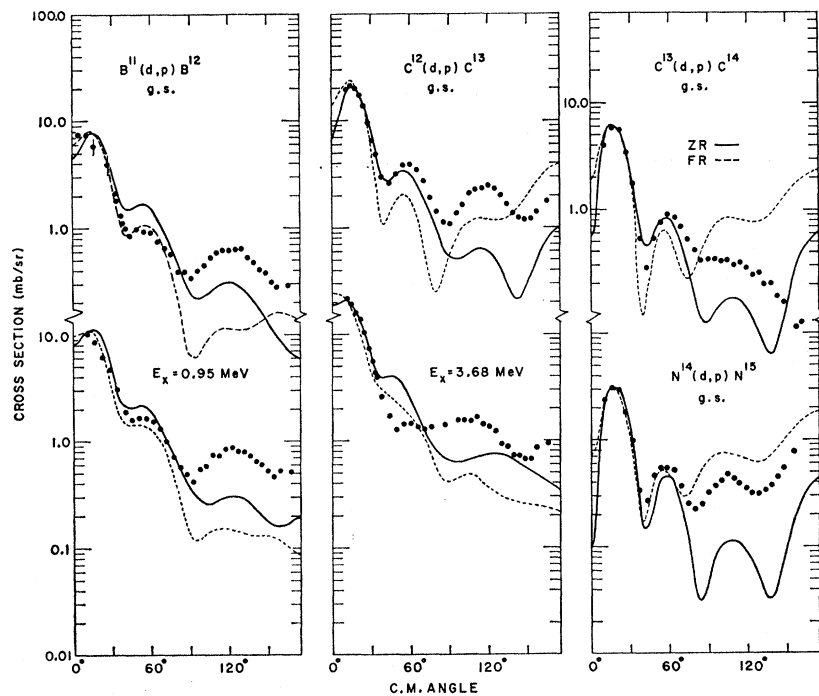


FIG. 3. Measured angular distributions of the  $(d,p)$  reactions to  $B^{11}$ ,  $C^{13}$ , and  $N^{14}$  at  $E_d = 12$  MeV. The lines represent DWBA calculations as described in the text. The solid lines are for zero range, the dashed for finite range (LEA).

### III. DISTORTED-WAVE BORN-APPROXIMATION CALCULATIONS

The elastic scattering of deuterons from light nuclei in this energy range has been studied systematically by the Heidelberg group,<sup>22</sup> who bombarded  $Be^9$ ,  $B^{10}$ ,  $B^{11}$ ,  $C^{12}$ ,  $N^{14}$ , and  $O^{16}$  with 11.8-MeV deuterons. Their work includes optical-model analyses in which the real well depth was kept fixed at 118 MeV and all other parameters, including the radial parameters for the surface-derivative imaginary potential, were varied for

a best fit to the data. Their parameters are based on those obtained by Satchler<sup>25</sup> from a similar study. No systematic trends with  $A$  are apparent in their best-fit parameters. For the purposes of the distorted-wave calculations, one is interested in average parameters. In particular, for the light nuclei it does not seem meaningful to use best-fit parameters that happen to reproduce the elastic scattering at just one energy since

<sup>25</sup> G. R. Satchler, private communications as quoted in P. E. Hodgson, *Advan. Phys.* **15**, 329 (1966).

TABLE I. Summary of experimental information.

Final nucleus	Excitation energy (MeV)	$Q$ (MeV)	$J^\pi$	$\theta_{\text{peak}}$ (deg)	$\sigma_{\text{peak}}$ (mb/sr)	$S_{\text{exp}}^a$
Li <sup>7</sup>	g.s.	5.03	$\frac{3}{2}^-$	18	9.37	0.90
	0.48	4.55	$\frac{1}{2}^-$	18	6.82	1.15
Li <sup>8</sup>	g.s.	-0.19	2 <sup>+</sup>	18	22.0	0.87
	0.98	-1.17	1 <sup>+</sup>	12	9.76	0.48
Be <sup>10</sup>	g.s.	4.59	0 <sup>+</sup>	15	3.38	1.67
	3.37	1.22	2 <sup>+</sup>	16	4.86	0.24
	6.18	-1.59	0 <sup>+</sup>	~10	(0.33) <sup>b</sup>	(0.045)
B <sup>11</sup>	g.s.	9.23	$\frac{3}{2}^-$	16	2.99	1.21
	4.46	4.77	$\frac{3}{2}^-$	22	1.74	0.27
	6.76	2.47	$\frac{7}{2}^-$	17	12.9	1.11
B <sup>12</sup>	g.s.	1.14	1 <sup>+</sup>	6-11	7.54	0.78
	0.98	0.16	2 <sup>+</sup>	11	10.4	0.54
	2.72	-1.58	(0 <sup>+</sup> ) <sup>c</sup>	15	(0.78) <sup>b</sup>	(0.12)
C <sup>13</sup>	g.s.	2.72	$\frac{1}{2}^-$	14	21.3	1.16
	3.68	-0.96	$\frac{3}{2}^-$	11	21.2	0.22
C <sup>14</sup>	g.s.	5.95	0 <sup>+</sup>	16	5.88	2.05
N <sup>15</sup>	g.s.	8.61	$\frac{1}{2}^-$	16	3.15	1.22

<sup>a</sup> Obtained in DWBA calculations with H parameters, zero range, 4-F cutoff, and appropriate admixtures of  $\Delta J = \frac{1}{2}$  and  $\frac{3}{2}$  (Table V).

<sup>b</sup> Only the cross section at the expected peak was measured—not the angular distribution.

<sup>c</sup> Spin assignment tentative (Ref. 31).

these may tend to vary from the average parameters for a variety of reasons (for instance, resonances in the compound nucleus). The average parameters would tend to smooth out such anomalies in the potentials. It is nevertheless true that such anomalies in individual nuclei would also effect the  $(d, p)$  reaction. Such effects, however, usually could not be reproduced by a simple Woods-Saxon potential of the type used in DWBA calculations, even if it were adjusted to fit the elastic data.

We have accordingly chosen to take the arithmetic mean of the Heidelberg type-I parameters (H) for our

TABLE II. Parameters used in DWBA calculations.<sup>a</sup>

	Incident particle (deuteron)			Captured particle (neutron)	Outgoing <sup>e</sup> particle (proton)
	Set H <sup>b</sup>	Set C <sup>c</sup>	Set HII <sup>d</sup>		
$V_0$ (MeV)	118	118	78		45
$r_0$ (F)	0.886	0.886	0.9	1.32	1.32
$r_c$ (F)	1.3	1.3	1.3		1.3
$a$ (F)	0.907	0.907	0.95	0.57	0.57
$V_{s0}$ (MeV)	5.8	5.8	5.8	$\Lambda = 25$	5.0
$W'$ (MeV)	5.8	6.3	30		11
$r_0'$ (F)	1.57	1.77	0.9		1.32
$a'$ (F)	0.777	0.66	0.8		0.345

<sup>a</sup> The notation is standard;  $V = V_0 f(r_0, a) - iWg(r_0', a')$ , where  $f = [1 + \exp[(r - r_0 A^{1/3})/a]]^{-1}$ ,  $g = df/dr$  (or  $= f$  for volume absorption). The value of  $W'$  was multiplied by 4 for the JULIE calculations.  $\Lambda$  is the spin-orbit parameter multiplying the usual Thomas term.

<sup>b</sup> Type I from Ref. 22.

<sup>c</sup> Reference 26.

<sup>d</sup> Type II from Ref. 22; volume absorption was used.

<sup>e</sup> Parameters are a reasonable average to those obtained for proton scattering on C<sup>12</sup> [J. S. Nodvik, C. B. Duke, and M. A. Melkanoff, Phys. Rev. 125, 975 (1962)], neutron scattering on Li, Be, B, L, and N [H. F. Lutz, J. B. Mason, and M. D. Karvelis, Nucl. Phys. 47, 521 (1963)], and proton scattering on Be<sup>9</sup> and B<sup>11</sup> [R. H. Siemssen (private communication)].

deuteron potential, and have used this *same* potential for all reactions studied. *A priori* there is no obvious justification for assuming that all light nuclei have the same average optical potential, differing only by the  $A^{1/3}$  dependence of their radii. However, we chose to make this rather simplifying assumption in order to have a clearly defined procedure for handling the DWBA calculations. These average parameters do not appreciably alter the quality of the fit to the elastic data of Ref. 22. As an alternative set of parameters, we chose a set found by Satchler<sup>26</sup> in fitting elastic deuteron scattering from carbon over a range of energies. The second set of parameters differs from the first mainly in the larger value of the imaginary radius. The parameters used are given in Table II.

The JULIE code was used for the calculations.<sup>27</sup> With the customary zero-range calculations, the shapes of the

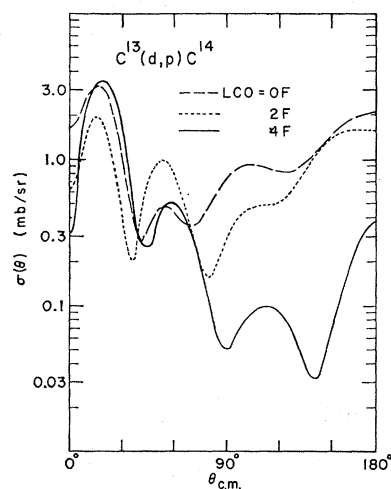


FIG. 4. Zero-range DWBA calculations with various cutoff radii as indicated.

angular distributions agreed very poorly with the experimental ones. A cutoff radius was tried and as is seen in Fig. 4 and Table III, it was found that the forward peak cross section first decreased and at 4 F reached approximately the same value as the zero-cutoff calculation. In this latter case, however, the shape of the calculated angular distribution was in much better agreement with experiment than before. Calculations were also made with form factors calculated by the local-energy approximation (LEA)<sup>28</sup> and results were in qualitative agreement with those obtained with zero range and a 4-F cutoff.

The differences between various types of calculations

<sup>26</sup> G. R. Satchler, Nucl. Phys. 85, 273 (1966).

<sup>27</sup> R. H. Bassel, R. M. Drisko, and G. R. Satchler, Oak Ridge National Laboratory Report No. ORNL-3240 (unpublished), and additions.

<sup>28</sup> J. K. Dickens, R. M. Drisko, F. G. Perey, and G. R. Satchler, Phys. Letters 15, 337 (1965). The parameters were:  $\beta = 0.85$  F for nucleons and 0.54 F for deuterons;  $r_0 = 1.25$  F.

are summarized in Table IV with the  $\pm$  values indicating the mean deviations from the averages given. As a general conclusion one can state that the peak cross sections did not change by more than an over-all uncertainty of  $\sim 15\%$  when (a) a cutoff radius of 4 F was compared with no cutoff, and (b) the local-energy approximation was tried and compared with zero range. However, calculations for the  $B^{10}(d,p)B^{11}$  reactions with the set-II Heidelberg (HII) parameters<sup>22</sup> indicate an average 40% increase in the calculated JULIE cross sections. The results therefore are sensitive to the choice of potentials. The calculations did, in general, reproduce the period of the oscillating structure in the angular distributions, but not the amplitude of the oscillations nor the general level of cross sections. No sign of the rather prominent  $J$  dependence found in the data (see Sec. V) was detected in the DWBA calculations. The 4-F zero-range calculations and those using the local-energy approximation (both with the H parameters) are plotted in Figs. 1-3 along with the data.

TABLE III. DWBA peak cross sections as a function of cutoff radius for  $C^{13}(d,p)C^{14}$ .

Lower cutoff radius (F)	$\sigma_{\text{peak}}$ (mb/sr) <sup>a</sup>	
	Zero-range approximation	Local-energy approximation
0	3.20	3.54 <sup>b</sup>
2	1.93	2.80
3	2.54	3.32
4	3.43 <sup>b</sup>	4.14
5	2.49	3.19

<sup>a</sup> The cross sections are from the JULIE code and are not corrected for the Hulthén wave function nor are statistical factors included.

<sup>b</sup> The italicized cross sections are the ones used in the analysis of the data.

#### IV. SPECTROSCOPIC FACTORS

Since the DWBA calculations for peak cross sections were relatively insensitive to the details of the assumptions (except for the drastic difference with the HII parameters), the zero-range calculations with the H parameters were chosen with a 4-F cutoff to carry out the analysis. These cross sections were multiplied by the factor of 1.65 to correct for Hulthén wave functions for the deuteron.<sup>29</sup> Spectroscopic factors were then obtained from the expression

$$S \equiv \frac{\sigma_{\text{expt}}(\text{peak})}{1.65[(2J+1)/(2I+1)]\sigma_{\text{JULIE}}(\text{peak})},$$

where  $I$  and  $J$  are the spins of the initial and final states, respectively.

These results can then be compared with spectroscopic factors obtained in the shell-model calculation of Cohen and Kurath,<sup>30</sup> in which effective interactions

<sup>29</sup> R. M. Drisko (private communication).

<sup>30</sup> S. Cohen and D. Kurath, Nucl. Phys. **73**, 1 (1965); **A101**, 1 (1967).

TABLE IV. Summary of variations between DWBA calculations. The  $\pm$  values in the last two columns are the mean fluctuations.

Parameters for deuteron potential	Range	Cutoff radius (F)	Difference between peak cross sections (%)	
			$(\sigma - \sigma_0)/\sigma_0^a$	$(\sigma_{3/2} - \sigma_{1/2})/\sigma_{3/2}^b$
H	0	4	...	10 $\pm$ 10
H	0	0	0 $\pm$ 10	
H	finite (LEA)	0	5 $\pm$ 7	4 $\pm$ 15
C	0	4	-6 $\pm$ 4	
HII	0	4	40 $\pm$ 8	

<sup>a</sup> The parameters for the deuteron potential used to calculate  $\sigma$  in each case are specified in the first three columns. The cross section  $\sigma_0$  was calculated with the parameters specified in line 1.

<sup>b</sup> The cross section  $\sigma_{3/2}$  was calculated for  $j = \frac{3}{2}$  transitions;  $\sigma_{1/2}$  is for  $j = \frac{1}{2}$  transitions.

were obtained in the 1p shell by fitting available data on energy levels. The spectroscopic factors derived from the data are given in Table I, those taken from Cohen and Kurath are given in Table V.

In making the comparison, the question remains: When is an absolute difference most significant? Ratios are clearly not very meaningful to compare because there is no way of separating weak transitions from strong ones. But what do we mean by weak or strong? We can take the view that we are testing theory (shell-model coupled to the DWBA) and compare experimental peak cross sections with calculated ones. This is done in Fig. 5(a). It is evident that the cross sections are especially large for the excited states in Li<sup>8</sup> or C<sup>13</sup> which have low  $Q$  values. If we take the view that we want to divide out "kinematic" effects, we can look

TABLE V. Summary of spectroscopic information.

Final nucleus	Experimental excitation of state (MeV)	$J^\pi$	$S_{\text{theor}}^a$	Fraction <sup>a</sup> of $\Delta J = \frac{3}{2}$	
				(%)	$S_{\text{exp}}/S_{\text{theor}}$
Li <sup>7</sup>	g.s.	$\frac{3}{2}^-$	0.721	60	1.24
	0.48	$\frac{1}{2}^-$	0.893	96	1.29
Li <sup>8</sup>	g.s.	2 <sup>+</sup>	1.033	95	0.84
	0.98	1 <sup>+</sup>	0.446	72	1.09
Be <sup>10</sup>	g.s.	0 <sup>+</sup>	2.357	100	0.71
	3.37	2 <sup>+</sup>	0.274	17	0.87
			0.194 <sup>b</sup>	65 <sup>b</sup>	1.22 <sup>b</sup>
B <sup>11</sup>	6.18	0 <sup>+</sup>	0.386 <sup>c</sup>	100 <sup>c</sup>	(0.12) <sup>c</sup>
	g.s.	$\frac{3}{2}^-$	1.094	100	1.11
	4.46	$\frac{1}{2}^-$	0.135	71	1.98
B <sup>12</sup>	6.76	$\frac{3}{2}^-$	0.877	6	1.26
	g.s.	1 <sup>+</sup>	0.826	14	0.95
	0.98	2 <sup>+</sup>	0.561	0.2	0.97
C <sup>13</sup>	2.72	(0 <sup>+</sup> ) <sup>d</sup>	0.398 <sup>c</sup>	100 <sup>c</sup>	(0.30) <sup>c</sup>
	g.s.	$\frac{1}{2}^-$	0.613	0	1.89
C <sup>14</sup>	3.68	$\frac{1}{2}^-$	0.188	100	1.19
	g.s.	0 <sup>+</sup>	1.734	0	1.18
N <sup>15</sup>	g.s.	$\frac{1}{2}^-$	1.459	2	0.84

<sup>a</sup> From Ref. 30.

<sup>b</sup> Parameters for the 2BME calculation of Ref. 30.

<sup>c</sup> Assignment of state to one within the 1p configuration may be dubious; the energies are in poor agreement.

<sup>d</sup> Spin assignment tentative (Ref. 31).

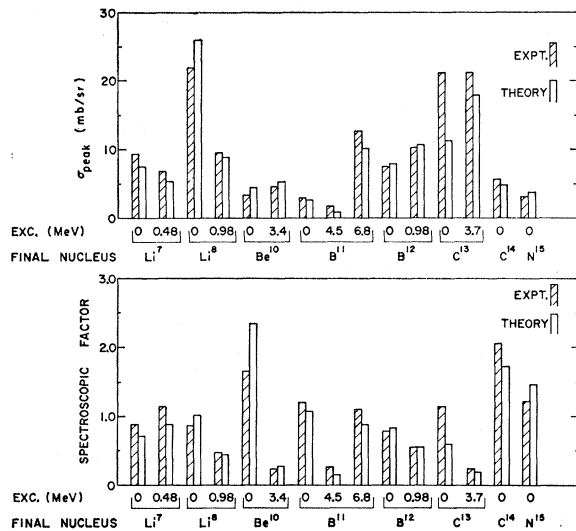


FIG. 5. Summary of experimental and theoretical results. The DWBA calculations are described in the text; the theoretical spectroscopic factors are those of Ref. 30. The results are displayed in the form of both peak cross sections and spectroscopic factors.

at a comparison of spectroscopic factors as in Fig. 5(b). The experimental/theoretical ratios are plotted against  $Q$  value in Fig. 6. The absence of a systematic trend with  $Q$  argues for the success of the DWBA.

In addition of the transitions discussed above, some data were obtained with the magnetic spectrograph for two transitions to  $0^+$  states which may belong within the  $1p$  configuration. In both cases the states are weak and only data at the extreme forward angles were obtained. The results are for the 6.18-MeV state of  $\text{B}^{10}$  ( $\sigma_{\text{peak}} \leq 0.3$  mb/sr) and the 2.72-MeV state in  $\text{B}^{12}$

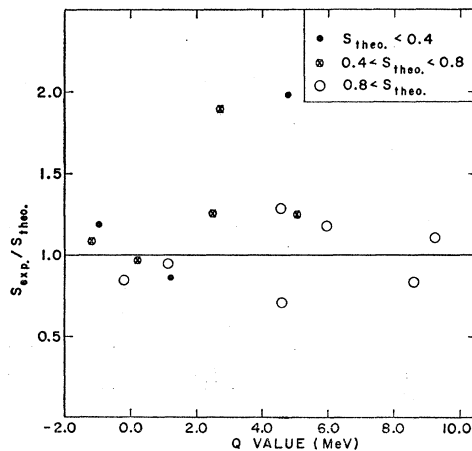


FIG. 6. Ratios of experimental measurements to theoretical predictions as a function of  $Q$  value. The two serious discrepancies are for the  $\text{C}^{12}(d,p)\text{C}^{13}$  g.s. reaction, and the rather weak  $\text{B}^{10}(d,p)\text{B}^{11}$  (4.46-MeV) transition.

( $\sigma_{\text{peak}} \leq 0.8$  mb/sr).<sup>31</sup> These peak cross sections correspond to  $S \leq 0.05$  and  $\leq 0.12$ , respectively. For the  $0^+$  states that might correspond to these, Cohen and Kurath calculated  $S=0.39$  and  $0.40$ , and their calculated energies are considerably higher than the experimental ones. These states then seem to contain rather large admixtures from higher configurations, possibly in analogy with the low-lying  $0^+$  state of  $\text{C}^{12}$ . Such admixtures would tend to account for the lower spectroscopic factors. It should be emphasized that the experimental numbers are upper limits, since we did not establish that the angular distributions for these states were  $l=1$ , and the identification of the states with ones expected from the shell-model calculation is dubious.

The relatively large discrepancy for the spectroscopic factor derived from the  $\text{B}^{10}(d,p)\text{B}^{11}$  reaction to the 4.46-MeV state is not particularly disturbing; since the theoretical spectroscopic factor for this transition is the smallest of those studied, its value might depend sensitively on details of the theoretical calculation.

Our  $\text{C}^{12}(d,p)\text{C}^{13}$  ground-state (g.s.) peak cross section of 21.3 mb/sr can be compared with the 20 mb/sr measured<sup>10</sup> at 11.8 MeV and<sup>32</sup> the 19.0 mb/sr at 12 MeV. All three are about double the theoretical value. The reason for this anomalous result in the  $\text{C}^{12}(d,p)\text{C}^{13}$  g.s. reaction may be associated with the fact that  $\text{C}^{12}$  is more tightly bound than the other nuclei studied. In fact, the excitation energy of the compound system  $\text{C}^{12}+d$  is  $\sim 5$  MeV lower than that of any of the other cases. Both the excitation function for the elastic scattering of deuterons<sup>33</sup> and the  $(d,p)$  reaction itself<sup>34</sup> exhibit

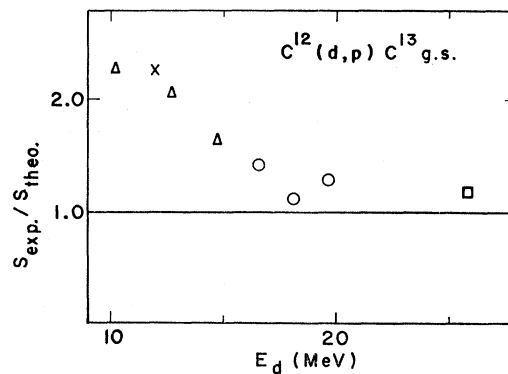


FIG. 7. Ratios of experimental to theoretical spectroscopic factors for the  $\text{C}^{12}(d,p)\text{C}^{13}$  (g.s.) reaction. The cross represents the present measurement, the triangles those of E. W. Hamburger [Phys. Rev. **123**, 619 (1961)], the circles those of Ref. 6, and the square that of Ref. 7.

<sup>31</sup> The  $0^+$  assignment for the 2.72-MeV state in  $\text{B}^{12}$  is rather tentative: A. Gallmann, F. Hibou, P. Fintz, P. E. Hodgson, and E. K. Warburton, Phys. Rev. **138**, B560 (1965).

<sup>32</sup> R. N. Glover and A. D. Jones, Nucl. Phys. **84**, 673 (1966).

<sup>33</sup> G. G. Ohlsen and R. E. Shamu, Nucl. Phys. **45**, 523 (1963).

<sup>34</sup> J. E. Evans, J. A. Kuehner, and E. Almqvist, Phys. Rev. **131**, 1632 (1963).

resonance structure up to  $\sim 11$  MeV, which is as high as these excitation functions have been measured. It therefore seems possible that resonance effects could account for the anomalously high peak cross section observed at 12 MeV for this reaction. This is also supported by analysis of data at other deuteron energies by use of the deuteron parameters of Ref. 26. In Fig. 7 we see these results converging to the expected value at  $E_d \gtrsim 16$  MeV.

### V. $J$ -DEPENDENT EFFECTS

Most of the target nuclei used in the present investigation do not have zero spin and therefore  $l=1$  transitions are not restricted to either  $\Delta J = \frac{1}{2}$  or  $\frac{3}{2}$  but are in general, a mixture of the two. For a prediction regarding probable admixtures we refer to Cohen and Kurath and, as can be seen from Table V, most of the transitions are characterized by one predominant  $J$  value. The angular distributions are replotted in Fig. 8, where they are separated on the basis of predominant  $J$  values. It is evident that the angular distributions for  $\Delta J \approx \frac{1}{2}$  have considerably more structure at backward angles than do those with  $\Delta J \approx \frac{3}{2}$ . The data on the Li isotopes do not show a consistent effect, though only the  $\text{Li}^6(d, p)\text{Li}^7$  g.s. transition is predicted to have a mixed transition with a  $\Delta J = \frac{1}{2}$  component as large as 40%. Possibly exchange effects, which are ignored in

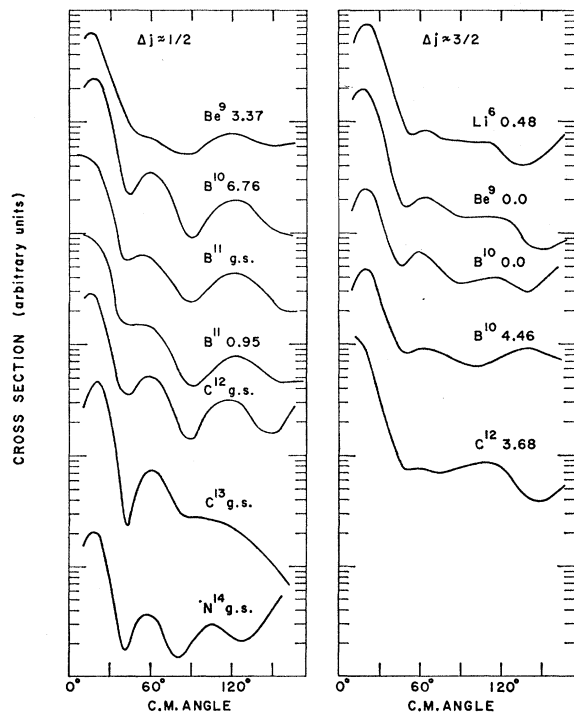


FIG. 8. Smooth lines drawn through the experimental angular distributions classified by dominant  $\Delta J$  according to Ref. 30. The data on three transitions on Li targets are not included.

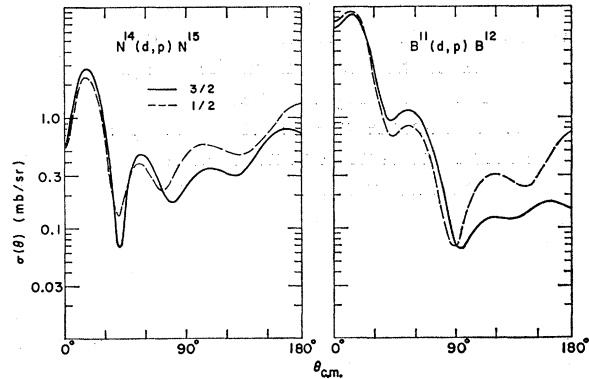


FIG. 9.  $J$  dependence in DWBA calculations (LEA) for two of the reactions studied. The parameters are the ones discussed in the text.

the DWBA treatment and should be most important for the lightest nuclei, perturb the angular distributions sufficiently at backward angles to cause the  $J$  dependence to be washed out. Alternatively, this may be another case of the recently reported dependence<sup>35</sup> on the final-state spin  $I$ . We had tried to use the depth of the persistent minimum at  $\sim 90^\circ$  as a measure of  $\frac{3}{2}$ - $\frac{1}{2}$  admixture and had some preliminary success,<sup>36</sup> but after the data for  $\text{C}^{13}(d, p)\text{C}^{14}$  and  $\text{N}^{14}(d, p)\text{N}^{15}$  were obtained, it was found that the position of the pronounced minimum seemed to shift between the first minimum ( $\sim 50^\circ$ ) and the second one ( $\sim 90^\circ$ ) with no appreciable change in reaction kinematics. We can only conclude that the presence of a pronounced minimum characterizes  $\Delta J = \frac{1}{2}$  and that any attempts to quantitatively predict admixtures from the shape of the angular distributions at this energy are questionable. It is not clear what properties of the reaction are responsible for the minimum in the angular distribution for  $\Delta J = \frac{1}{2}$ .

The optical parameters in the DWBA calculations included reasonable spin-orbit forces but, as in heavier nuclei, the calculated  $J$  dependence does not even qualitatively reproduce the observed one—as can be seen in Fig. 9.

### VI. DISCREPANCY BETWEEN $(\text{He}^3, d)$ AND $(d, n)$

Recently, discrepancies in relative spectroscopic factors were found for  $(\text{He}^3, d)$  and  $(d, n)$  reactions leading to states with different isobaric spin within the same final nuclei.<sup>37</sup> If normalized to the spectroscopic

<sup>35</sup> R. H. Siemssen and D. Dehanard, Phys. Rev. Letters **19**, 377 (1967).

<sup>36</sup> G. C. Morrison, J. P. Schiffer, R. H. Siemssen, and B. Zeidman, in *Proceedings of the International Conference on Nuclear Physics, Gallinburg, Tennessee, 1966* (Academic Press Inc., New York, 1967).

<sup>37</sup> R. H. Siemssen, G. C. Morrison, B. Zeidman, and H. Fuchs, Phys. Rev. Letters **16**, 1050 (1966).

factor of the  $T_{<}$  ground state, it was found that the  $(d,n)$  spectroscopic factors for the  $T_{>}$  states were consistently smaller than those from the  $(\text{He}^3,d)$  reaction. The  $(d,p)$  reaction being the analog to the  $(d,n)$ , it is of interest to examine whether or not the present data show related systematic deviations. As can be seen from Table V, there is no evidence for such effects in the  $(d,p)$  data. The absolute spectroscopic factor for the  $\text{Be}^9(d,p)\text{Be}^{10}$  g.s. reaction is somewhat too small, but that for  $\text{C}^{13}(d,p)\text{C}^{14}$  agrees very well with theory. The  $\text{Be}^9(d,p)\text{Be}^{10}$  and  $\text{C}^{13}(d,p)\text{C}^{14}$  reactions lead to the analog of the states for which the discrepancies between  $(\text{He}^3,d)$  and  $(d,n)$  were observed. No systematic deviations are found between the spectroscopic factors for transitions to  $T=\frac{1}{2}$  final states (all transitions to odd- $A$  final nuclei) and those for  $T=1$  final states (transitions to even- $A$  final nuclei).

Tamura<sup>38</sup> has shown that the  $(\text{He}^3,d)-(d,n)$  discrepancy is very likely due to the coupling between the neutron and the charge-exchange proton channel, similar to the coupling observed by Moore *et al.*<sup>39</sup> in the  $\text{Zr}^{90}(d,p)\text{Zr}^{91}$  reaction. Calculations by Tamura show that these effects are strongest at low bombarding energies [e.g., for the  $\text{Be}^9(d,n)\text{B}^{10}$  reaction the discrepancy is a factor of 2 at 5 MeV and is negligible at 15 MeV] and that they are more important for the  $(d,n)$  reaction than for the  $(d,p)$ . Since the  $(d,p)$  reaction always leads to the states for which the analog channel exists, the effects of the charge-exchange coupling should be present in all of the reactions that have been studied in the present work. The closeness of the over-all agreement between predicted and measured spectroscopic factors in the present investigation suggests that either the effects of the coupling on the  $(d,p)$  reaction at 12 MeV are negligible, or that our choice of the distorting parameters led to an accidental cancellation of these effects by predicting systematically too low DWBA cross sections.

<sup>38</sup> Taro Tamura, *Phys. Rev. Letters* **19**, 321 (1967).

<sup>39</sup> C. F. Moore, C. E. Watson, S. A. A. Zaidi, J. J. Kent, and J. G. Kulleck, *Phys. Rev. Letters* **17**, 926 (1966).

## VII. CONCLUSION

The  $(d,p)$  reaction in light nuclei seems to give, on the whole, surprisingly good agreement with shell-model calculations. This must be interpreted as a success of both the shell-model theory and the DWBA calculation with average distorting parameters. As we have seen, the choice of the "correct" family of optical potentials is fairly important; the ones originating with Satchler and having  $V \approx 118$  MeV,  $r_0 \approx 0.9$  F, and surface absorption with  $r_I \approx 1.5$  F seem to work. The DWBA fits are successful not only in peak cross sections but also in the more detailed structure at backward angles. Most of the positions of maxima and minima are correctly reproduced, though the amplitudes of oscillations and the  $J$  dependence usually are not reproduced. Only in the  $\text{C}^{12}(d,p)\text{C}^{13}$  g.s. reaction is there a pronounced discrepancy, possibly because of resonance effects.  $J$ -dependent effects in the  $1p$  shell seem to be as pronounced as they were in the  $2p$  shell. A systematic study of the  $(p,d)$  reaction, with the bombarding energies adjusted to give deuterons of comparable energies, should be a useful way of obtaining additional information on these nuclei—as would be studies of other stripping and pickup reactions.

## ACKNOWLEDGMENTS

We would like to thank J. R. Wallace and the operating group for the ANL tandem Van de Graaff for their cooperation in running the accelerator and E. J. Leech and W. Horath for technical help in connection with setting up the experiment and preparation of targets. We are very much indebted to Dr. Drisko, Dr. Satchler, Dr. Bassel, Dr. Dickens, and Dr. Pery for permitting us to use their computer codes. We would also like to thank Dr. Dieter Kurath for many helpful discussions.

## APPENDIX

The experimental cross sections for  $(d,p)$  reactions are given in Table VI following.

TABLE VI. Experimental cross sections for (d, p) reactions on Li<sup>6</sup>, Li<sup>7</sup>, Be<sup>9</sup>, B<sup>10</sup>, B<sup>11</sup>, C<sup>12</sup>, C<sup>13</sup>, and N<sup>14</sup>, measured at E<sub>d</sub>=12.0 MeV, except for Be<sup>9</sup>.

Li <sup>6</sup> (d, p)Li <sup>7</sup> , E <sub>x</sub> =0.0 MeV		Li <sup>6</sup> (d, p)Li <sup>7</sup> , E <sub>x</sub> =0.48 MeV		Li <sup>7</sup> (d, p)Li <sup>8</sup> , E <sub>x</sub> =0.0 MeV		Be <sup>9</sup> (d, p)Be <sup>10</sup> , E <sub>x</sub> =0.0 MeV (E <sub>d</sub> =11.8 MeV) <sup>a</sup>	
θ <sub>c.m.</sub> (deg)	σ <sub>c.m.</sub> (mb/sr)	θ <sub>c.m.</sub> (deg)	σ <sub>c.m.</sub> (mb/sr)	θ <sub>c.m.</sub> (deg)	σ <sub>c.m.</sub> (mb/sr)	θ <sub>c.m.</sub> (deg)	σ <sub>c.m.</sub> (mb/sr)
11.7	7.32	11.8	4.88	11.9	18.56	11.3	2.69
17.6	9.37	17.7	6.82	17.8	21.98		(2.82) <sup>b</sup>
23.4	9.05	23.5	6.75	23.8	17.98	14.5	3.38
29.3	6.55	29.3	4.86	29.7	11.49	16.0	3.30
35.0	3.75	35.1	2.95	35.5	8.12	16.8	(3.26) <sup>b</sup>
40.8	2.18	40.9	1.71	41.3	5.07	20.0	3.16
46.5	1.25	46.6	1.03	47.1	3.32	22.5	2.81
52.1	1.01	52.3	0.72	52.8	2.62		(2.90) <sup>b</sup>
57.7	1.20	57.9	0.75	58.5	2.58	28.0	2.01
63.3	1.23	63.4	0.78	64.0	2.09	33.6	1.09
68.7	1.32	68.9	0.76	69.6	1.66	39.1	0.56
74.2	1.19	74.3	0.67	75.0	1.64	44.6	0.32
79.5	1.17	79.7	0.63	80.4	1.33	50.1	0.30
84.8	1.04	90.1	0.63	85.7	1.60	55.5	0.33
90.0	1.04	95.3	0.58	90.9	1.45	60.9	0.36
95.1	1.03	100.3	0.57	96.0	1.45	66.2	0.36
105.1	1.09	105.3	0.60	101.1	1.27	71.5	0.33
110.0	1.08	110.1	0.61	106.0	1.22	76.7	0.28
114.8	1.00	114.9	0.59	110.9	1.30	82.0	0.26
119.5	0.94	119.7	0.48	115.7	1.26	87.1	0.24
128.7	0.93	124.3	0.45	120.4	1.34	92.2	0.24
133.3	0.89	128.9	0.39	125.0	1.28	97.2	0.23
137.7	0.93	133.4	0.38	129.6	1.26	102.2	0.25
142.1	0.98	137.9	0.37	134.0	1.32	107.1	0.23
146.5	1.01	142.3	0.39	138.5	1.33	112.0	0.24
150.8	1.09	146.6	0.42	142.8	1.39	116.8	0.23
155.0	1.14	150.9	0.48	147.1	1.56	121.5	0.25
159.3	1.20	155.1	0.50	151.3	1.67	126.2	0.21
167.6	1.13	159.3	0.58	155.5	1.66	130.9	0.19
		167.7	0.72	159.7	2.19	135.5	0.16
						140.1	0.13
						144.6	0.12
						149.1	0.12
						153.6	0.12
						158.0	0.12
						162.5	0.14
						166.9	0.14
B <sup>10</sup> (d, p)B <sup>11</sup> , E <sub>x</sub> =6.78 MeV <sup>c</sup>		B <sup>11</sup> (d, p)B <sup>12</sup> , E <sub>x</sub> =0.0 MeV		B <sup>11</sup> (d, p)B <sup>12</sup> , E <sub>x</sub> =0.95 MeV		C <sup>12</sup> (d, p) C <sup>13</sup> E <sub>x</sub> =0.0 MeV	
θ <sub>c.m.</sub> (deg)	σ <sub>c.m.</sub> (mb/sr)	θ <sub>c.m.</sub> (deg)	σ <sub>c.m.</sub> (mb/sr)	θ <sub>c.m.</sub> (deg)	σ <sub>c.m.</sub> (mb/sr)	θ <sub>c.m.</sub> (deg)	σ <sub>c.m.</sub> (mb/sr)
11.2	10.2	5.6	7.54	11.2	10.40	11.0	19.54
16.8	12.9	11.2	7.54	16.8	8.81	14.3	21.32
22.4	10.6	16.8	5.90	22.4	6.24	17.6	20.19
27.9	6.99	27.8	3.39	28.0	4.82	20.9	17.07
33.5	3.74	33.4	2.16	33.5	3.10	24.2	13.80
39.0	1.61	34.5	1.83	39.0	1.87	27.5	9.44
44.5	1.04	37.8	1.31	41.2	1.82	30.7	6.58
49.9	1.21	38.9	1.14	44.5	1.58	33.5	4.75
55.3	1.53	41.1	1.00	50.0	1.64	37.8	2.95
60.7	1.65	44.3	0.84	55.4	1.64	43.7	2.60
66.0	1.46	49.8	0.98	60.8	1.53	49.1	3.17
71.3	1.28	55.2	0.94	66.1	1.31	54.5	3.80
76.6	0.92	60.5	0.91	71.4	1.01	59.8	3.88
81.7	0.64	65.8	0.75	76.6	0.72	65.0	3.45
86.9	0.49	71.1	0.65	81.8	0.56	70.3	2.76
92.0	0.43	76.3	0.57	86.9	0.49	75.5	1.89
97.0	0.49	81.5	0.39	92.0	0.41	80.6	1.41
102.0	0.62	86.6	0.39	97.0	0.54	85.7	1.13
106.9	0.75	91.7	0.34	102.0	0.58	90.8	1.08
111.7	0.86	96.7	0.40	106.9	0.74	95.8	1.39
116.6	0.88	101.7	0.45	111.8	0.73	100.8	1.65
121.3	0.92	106.6	0.53	116.6	0.84	105.7	2.08
126.0	0.95	111.5	0.59	121.4	0.86	110.6	2.26
130.7	0.90	116.3	0.62	126.1	0.80	115.5	2.32
135.3	0.79	121.1	0.62	130.8	0.79	120.3	2.46
139.9	0.66	125.8	0.63	135.4	0.73	125.0	2.32
144.5	0.61	130.5	0.64	140.0	0.64	129.8	2.00
149.0	0.51	135.2	0.53	144.5	0.60	134.5	1.66
153.5	0.47	139.8	0.48	149.0	0.52	139.1	1.37
157.9	0.45	144.3	0.41	153.5	0.46	143.7	1.22
162.4	0.45	148.9	0.38	158.0	0.52	148.3	1.19
		153.4	0.31	166.8	0.51	152.9	1.20
		157.8	0.28			157.5	1.42
		166.7	0.29			166.5	2.21

